AMERICAN SOCIETY FOR MICROBIOLOGY | Applied and Environmental Microbiology®

Assessment of Soil Features on the Growth of Environmental Nontuberculous Mycobacterial Isolates from Hawai'i

Cody M. Glickman,[a] Ravleen Virdi,[a] Nabeeh A. Hasan,[a] L. Elaine Epperson,[a] Leeza Brown,[b] Stephanie N. Dawrs,[a] James L. Crooks,[c] Edward D. Chan,[d,e,f] Michael Strong,[a] Stephen T. Nelson,[b] Jennifer R. Honda[a]

aCenter for Genes, Environment and Health, National Jewish Health, Denver, Colorado, USA
bDepartment of Geological Sciences, Brigham Young University, Provo, Utah, USA
cDivision of Biostatistics and Bioinformatics, National Jewish Health, Denver, Colorado, USA
dMedicine and Academic Affairs, National Jewish Health, Denver, Colorado, USA
eDivision of Pulmonary Sciences and Critical Care Medicine, University of Colorado Anschutz Medical Campus, Aurora, Colorado, USA
fDepartment of Medicine, Rocky Mountain Regional Veterans Affairs Medical Center, Denver, Colorado, USA

Cody M. Glickman and Ravleen Virdi contributed equally to this work. Author order was determined alphabetically.

ABSTRACT Environmental nontuberculous mycobacteria (NTM), with the potential to cause opportunistic lung infections, can reside in soil. This might be particularly relevant in Hawai'i, a geographic hot spot for NTM infections and whose soil composition differs from many other areas of the world. Soil components are likely to contribute to NTM prevalence in certain niches as food sources or attachment scaffolds, but the particular types of soils, clays, and minerals that impact NTM growth are not well-defined. Hawai'i soil and chemically weathered rock (saprolite) samples were examined to characterize the microbiome and quantify 11 mineralogical features as well as soil pH. Machine learning methods were applied to identify important soil features influencing the presence of NTM. Next, these features were directly tested *in vitro* by incubating synthetic clays and minerals in the presence of *Mycobacteroides abscessus* and *Mycobacterium chimaera* isolates recovered from the Hawai'i environment, and changes in bacterial growth were determined. Of the components examined, synthetic gibbsite, a mineral form of aluminum hydroxide, inhibited the growth of both *M. abscessus* and *M. chimaera*, while other minerals tested showed differential effects on each species. For example, *M. abscessus* (but not *M. chimaera*) growth was significantly higher in the presence of hematite, an iron oxide mineral. In contrast, *M. chimaera* (but not *M. abscessus*) counts were significantly reduced in the presence of birnessite, a manganese-containing mineral. These studies shed new light on the mineralogic features that promote or inhibit the presence of Hawai'i NTM in Hawai'i soil.

IMPORTANCE Globally and in the United States, the prevalence of NTM pulmonary disease—a potentially life-threatening but underdiagnosed chronic illness—is prominently rising. While NTM are ubiquitous in the environment, including in soil, the specific soil components that promote or inhibit NTM growth have not been elucidated. We hypothesized that NTM culture-positive soil contains minerals that promote NTM growth *in vitro*. Because Hawai'i is a hot spot for NTM and a unique geographic archipelago, we examined the composition of Hawai'i soil and identified individual clay, iron, and manganese minerals associated with NTM. Next, individual components were evaluated for their ability to directly modulate NTM growth in culture. In general, gibbsite and some manganese oxides were shown to decrease NTM, whereas iron-containing minerals were associated with higher NTM counts. These data provide new information to guide future analyses of soil-associated factors impacting persistence of these soil bacteria.

N atural and human-made environments harbor potentially disease-causing species of nontuberculous mycobacteria (NTM) (1). The NTM species responsible for human lung infections are thought to be influenced by the specific environmental source exposures and the NTM species diversity within these environmental niches. While water-associated biofilms contain potentially disease-causing NTM, a variety of NTM species have also been discovered in soil (2–4). Prior studies have shown that potting soil can be a reservoir for clinically relevant mycobacteria (4). In Japan, residential soil from patients with pulmonary NTM infections were demonstrated to harbor NTM that were genetically related to patients' respiratory NTM isolates, and that soil was a source of the patients' polyclonal and mixed *Mycobacterium avium* complex infections (5, 6). In the United States, Hawai'i has the highest prevalence of NTM lung infections, with almost four times higher NTM infection rates than the national average in a survey among older adults (7). In prior work (8), we reported the presence of clinically relevant slow-growing mycobacteria (SGM), including *Mycobacterium chimaera*, *Mycobacterium marseillense*, and *Mycobacterium intracellulare*, in Hawai'i soil samples, in addition to rapid-growing mycobacteria (RGM), including *Mycolicibacterium septicum* and *Mycolicibacterium alvei*.

The breadth of NTM species diversity in soil is likely driven by the proportion and composition of minerals and nutrients in that particular soil sample. For example, larger amounts of metals such as copper and cations such as sodium have been shown to be significant predictors for NTM infection in the United States. (9). Prior studies from Queensland, Australia, have shown soil containing nutrients such as nitrate or having low pH predicted the presence of RGM, including *Mycolicibacterium fortuitum* and *Mycobacteroides chelonae* (10). Yet soil components such as natural rock, sand, and clay may also impact NTM presence and diversity. A study by Lipner et al. reported increasing clay concentrations as protective against NTM, while increasing silt concentrations were associated with NTM infection (11). In this same study and another, a higher manganese concentration was associated with disease prevalence (9, 11). Thus, variable soil characteristics and components may either inhibit or promote NTM growth in soil.

In the current study, we performed microbiome and mineral/chemical analyses on a set of Hawai'i soil samples and tested the impact of particular clays and chemicals on the *in vitro* growth of native NTM species recovered from the Hawai'i environment. Since almost all of the rock underlying Hawai'i ecosystems is oceanic basalt comprised of volcanic rock with limited variations in composition (12), the characteristics associated with the presence of NTM in Hawai'i soil may significantly vary from what has been described so far.

RESULTS

Less diverse microbiome in NTM culture-positive soil samples. Of the total soil samples from this study, a subset ($n = 18$, comprised of 8 NTM culture positive and 10 NTM culture negative) were subjected to exploratory microbiome analyses. Linear modeling of mycobacterium genus counts against pH and culture status revealed no significant relationships ($F = 1.007$ and $P = 0.330$ and $F = 1.119$ and $P = 0.306$, respectively). The Shannon diversity index was used to compare species richness between NTM culture-positive and NTM culture-negative groups. The Shannon diversity values between NTM culture groups showed a trend toward significance, with NTM culture-positive samples having a lower overall diversity than NTM culture-negative samples (Fig. S4A in the supplemental material). Taxonomic analysis revealed the phylum *Firmicutes* was significantly enriched in NTM culture-positive samples (Fig. S4B) and the phylum composition varied by culture status (Fig. S4C). Similar trends in Shannon diversity and overall phyla abundance were also observed when the data were stratified by mycobacteria genus counts (Fig. S5A and B).
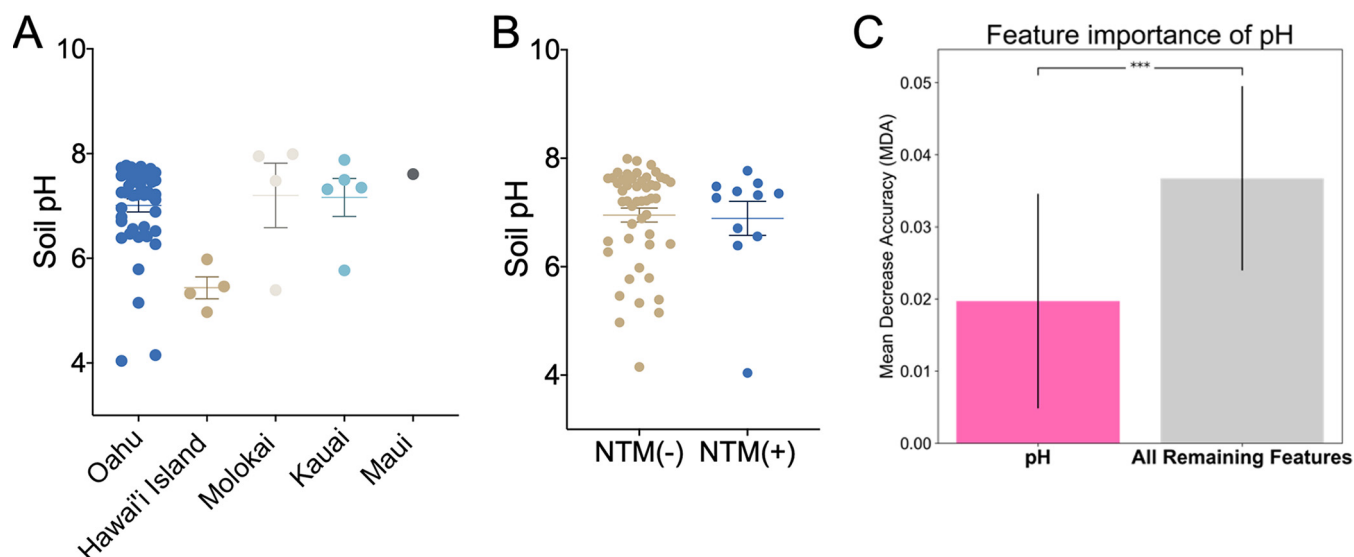
FIG 1 NTM culture results are not related to soil pH. (A) pH was measured from soil samples collected from Oahu ($n = 46$), Hawai'i Island ($n = 4$), Molokai ($n = 4$), Kauai ($n = 5$), and Maui ($n = 1$). pH value distributions were plotted by island and tested for differences (one-way ANOVA; *, $P = 0.01$). (B) Soil samples were stratified by NTM culture status, and all pH values are plotted. NTM culture-negative samples, pH mean = 6.95 ($n = 49$); NTM culture-positive samples, pH mean = 6.89 ($n = 11$) (one-way ANOVA; not significant; $P = 0.85$). (C) Feature importance is defined by mean decrease in accuracy (MDA) after 1,000 iterations of a classifier while shuffling the feature values. A higher MDA is associated with an important feature in the model. All remaining features is an average of the importance and variation among features other than pH. The importance of pH is lower than the average of all remaining features (0.0197 ± 0.0145 versus 0.0367 ± 0.0128; ***, $P < 0.0001$).

NTM recovery is not driven by soil pH. Soil was subjected to pH analyses. Overall, there was a statistically significant difference in soil pH among the individual islands. Specifically, of the five islands examined, the pH of Hawai'i Island soil was more acidic (mean pH = 5.4) than the soil pH of 7.1 to 7.6 of the other four islands (Fig. 1A). However, pH did not significantly vary when the data were stratified by NTM culture results (Fig. 1B). Compared to an average of all other features in the data set, the importance of pH as a feature had a lower mean decrease in accuracy (Fig. 1C).

Gibbsite, a clay mineral, inhibits both *M. abscessus* and *M. chimaera in vitro*. Exploratory feature importance selection was then performed against the full data set to elucidate possible clay characteristics that correlate to the presence of NTM. Based on our feature prediction models, gibbsite (a clay mineral) and 1:1 clays (a group of structurally related minerals where the fundamental building block consists of a sheet of silicate tetrahedra bonded to a layer of Al-O-OH or Mg-O-OH octahedra, which includes kaolinite and halloysite, the most common 1:1 clays in Hawai'i) (13, 14) were predicted to be less important compared to all other features in the data set (Fig. 2A). Alternatively, based again on our machine learning models, NTM culture-negative samples were predicted to have more gibbsite and 1:1 clays when stratified by culture status (Fig. S6A). To directly test these hypotheses, gibbsite and the clays kaolin and halloysite were incubated separately in the presence of NTM. Synthetic gibbsite significantly inhibited the growth of both *M. abscessus* and *M. chimaera in vitro* (Fig. 2B and C), as well as *M. avium*, at 48 h (Fig. S7A) compared to the untreated controls. The growth of *M. abscessus* and *M. chimaera* was not significantly altered by exposure to kaolin or halloysite (Fig. 2B and C), but halloysite significantly facilitated the growth of *M. avium* at 96 h (Fig. S7A).

To investigate whether the aforementioned results could be replicated using actual soil samples, three Hawai'i soil samples were identified to contain (i) 100% kaolinite (Honolulu [HNL] sample 12-48), (ii) 35% halloysite/27% gibbsite (rappelling sample 2-2 [RAP2-2]), or (iii) 55% halloysite (RAP2-5). Similar to Fig. 2B, the growth of *M. abscessus* was not impacted when cocultured with HNL 12-48, a soil comprised of 100% kaolinite (Fig. 2D); in contrast, significantly less *M. chimaera* was recovered (Fig. 2E). The inhibitory effect of gibbsite on NTM growth was lost when incubated with soil con-
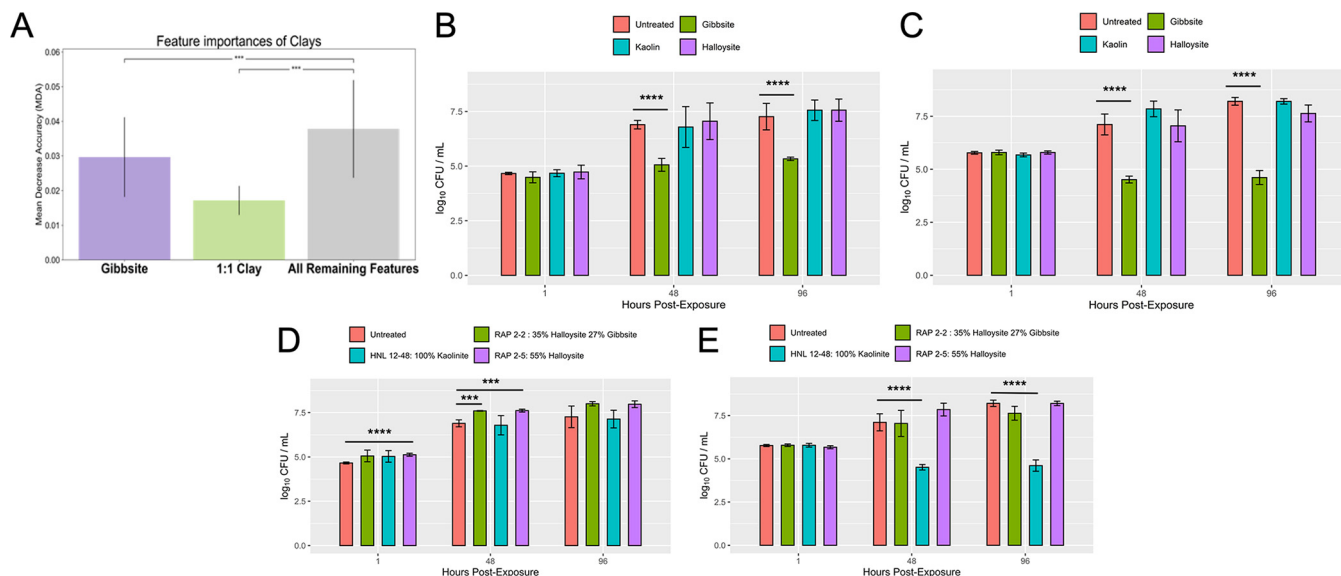
FIG 2 Impact of clay minerals on the *in vitro* growth of native Hawai'i environmental NTM isolates. (A) Distribution of clay mineral mean decrease in accuracy across 1,000 iterations of shuffling. The importance of gibbsite is less than the average of the remaining features (0.0302 ± 0.0117 versus 0.0377 ± 0.0141). However, the importance of gibbsite is greater than 1:1 clay (0.0302 ± 0.0117 versus 0.0172 ± 0.0041). (B) *In vitro* growth of *M. abscessus* in the presence of synthetic gibbsite, kaolin, and halloysite. (C) *In vitro* growth of *M. chimaera* in the presence of synthetic gibbsite, kaolin, or halloysite. (D) *In vitro* growth of *M. abscessus* in the presence of Hawai'i soil. (E) *In vitro* growth of *M. chimaera* in the presence of Hawai'i soil. ***, $P < 0.001$; ****, $P < 0.0001$.

taining both gibbsite and halloysite (Fig. 2D and E). *M. abscessus* showed significantly higher growth early after exposure to RAP2-5 (1 and 48 h) and RAP2-2 soil samples (48 h); however, incubation with these soils did not affect *M. chimaera* growth *in vitro* compared to the bacteria alone group (untreated) (Fig. 2D and E).

Iron minerals significantly increase NTM growth *in vitro*. Based on our feature prediction modeling, iron oxide minerals such as maghemite, hematite, and magnetite are posited to be of greater importance than the combination of all remaining features (Fig. 3A). To estimate the directionality of maghemite, hematite, and magnetite to NTM growth, the amounts of these iron oxides in each soil sample were plotted against NTM culture status, predicting more hematite and maghemite in NTM-positive cultures (Fig. S6B). Tested *in vitro*, the growth of *M. abscessus* was generally significantly enhanced in the presence of hematite and maghemite compared to the untreated control (Fig. 3B). While greater counts of *M. chimaera* were observed for all iron oxides tested at the 24-h mark than the untreated control (Fig. 3C), growth decreased at the 48-h time point in the samples incubated with maghemite and magnetite (Fig. 3C). However, CFU abundance in the samples was equivalent by the 96-h time point for all *M. chimaera* samples.
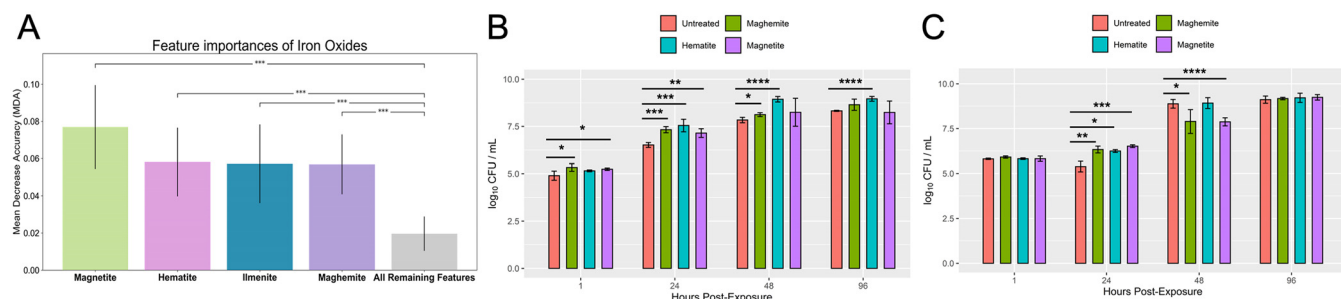

FIG 3 Impact of iron minerals on the *in vitro* growth of native Hawai'i environmental NTM isolates. (A) Distribution of iron oxide mean decrease in accuracy across 1,000 iterations of shuffling. The lowest iron oxide mineral (maghemite) is greater than the average of all remaining features, suggesting iron oxide minerals are important for NTM growth (0.0569 ± 0.0160 versus 0.0196 ± 0.0092). Magnetite is of greater importance than maghemite (0.0770 ± 0.0226 versus 0.0569 ± 0.0160) or hematite (0.0770 ± 0.0226 versus 0.0581 ± 0.0185). (B) *In vitro* growth of *M. abscessus* in the presence of synthetic maghemite, magnetite, and hematite. (C) *In vitro* growth of *M. chimaera* in the presence of synthetic maghemite, magnetite, and hematite. *, $P < 0.05$; **, $P < 0.01$; ***, $P < 0.001$; ****, $P < 0.0001$.
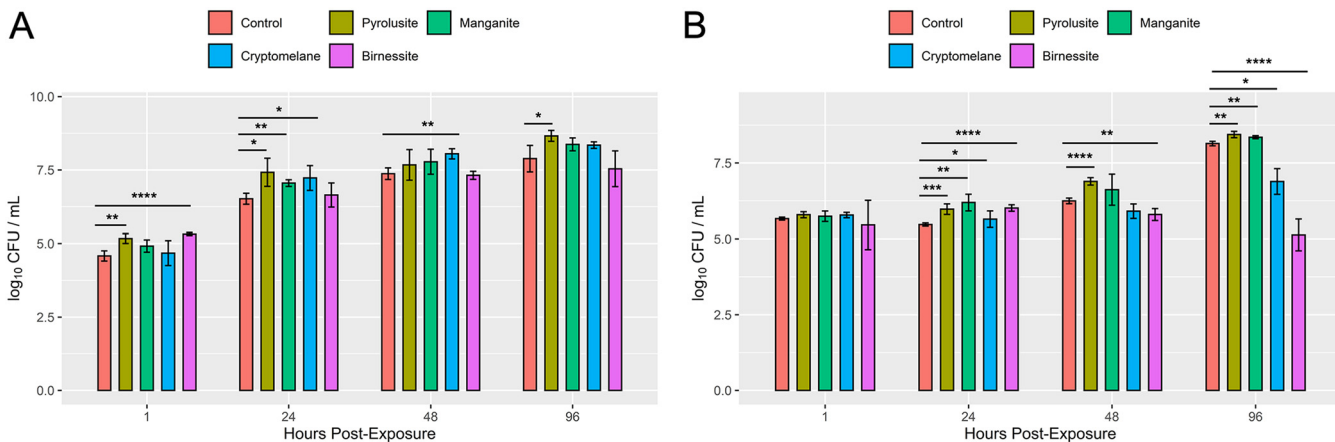
FIG 4 Impact of a manganese compound on the *in vitro* growth of native Hawai'i environmental NTM isolates. *In vitro* growth of *M. abscessus* (A) or *M. chimaera* (B) in the presence of synthetic manganese minerals. *, $P < 0.05$; **, $P < 0.01$; ***, $P < 0.001$; ****, $P < 0.0001$.

Similar to *M. abscessus*, significantly more *M. avium* was observed when incubated with hematite (Fig. S7B).

Manganese minerals show varied effects on NTM growth *in vitro*. Because soil manganese has been associated with a lower risk for NTM infections (7, 9), the effects of manganese minerals on NTM growth were tested. *M. abscessus*, *M. chimaera*, and *M. avium* were incubated in the presence of manganese minerals, including synthetic pyrolusite, manganite, cryptomelane, and birnessite. Results were varied. In general, the growth of all NTM tested was significantly higher when cultured in the presence of the manganese oxide pyrolusite (Fig. 4A and B; Fig. S7). While the growth of *M. abscessus* was also higher in the presence of cryptomelane (24 and 48 h), *M. chimaera* growth was significantly inhibited by the 96-h time point. Less *M. chimaera* was also observed in the presence of the manganese oxide mineral birnessite. Of importance, birnessite also significantly inhibited the growth of *M. avium* (Fig. S7C) while showing little effect on *M. abscessus* viability.

Pictorial of NTM attachment to mineral surfaces. *In vitro* assays demonstrated more numbers of *M. abscessus* and *M. chimaera* in the presence of hematite, whereas gibbsite and birnessite significantly inhibited the growth of NTM. Scanning electron microscopy (SEM) images show *M. abscessus* (Fig. 5A) and *M. chimaera* (Fig. 5B) alone
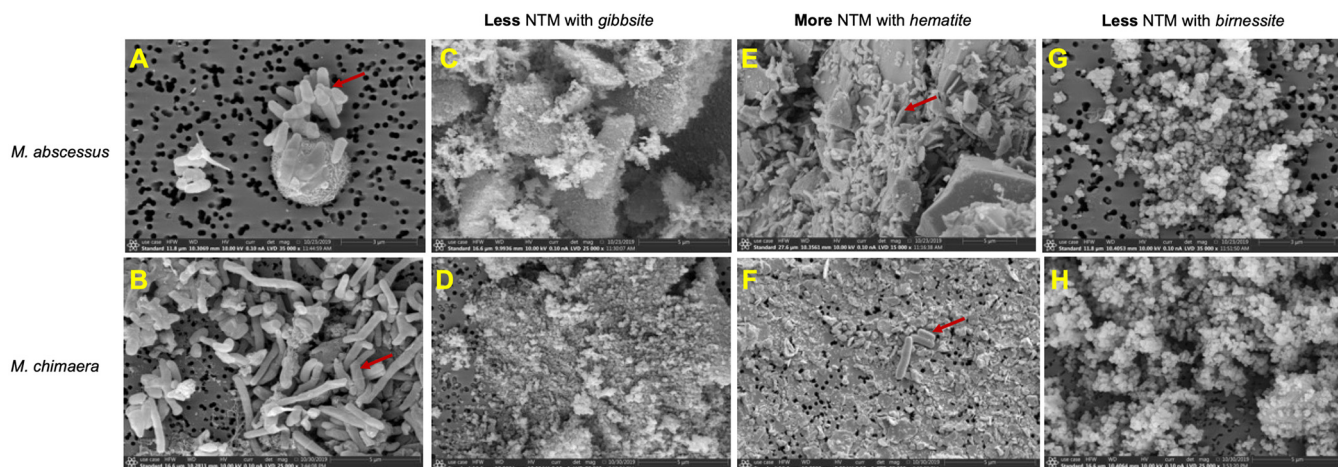
FIG 5 Scanning electron microscope images of environmental NTM isolates grown in the presence of gibbsite, hematite, and birnessite. *M. abscessus* (3 μm) (A) and *M. chimaera* (5 μm) (B) in the absence of soil minerals. *M. abscessus* (C) and *M. chimaera* (D) in the presence of gibbsite. *M. abscessus* (E) and *M. chimaera* (F) in the presence of hematite. *M. abscessus* (G) and *M. chimaera* (H) in the presence of birnessite. Red arrows indicate the NTM bacilli.

and in association with hematite (Fig. 5E and F), whereas no bacilli are seen in the presence of gibbsite (Fig. 5C and D) and birnessite (Fig. 5G and H).

DISCUSSION

Infections due to NTM are a growing clinical concern across the United States and many parts of the world due to their increasing prevalence and their recalcitrant nature to current chemotherapeutic treatments. It is widely recognized that environmental exposures contribute to NTM acquisition. While not as widely sampled or well characterized as water-associated biofilms, NTM occupy soil niches globally. Because 80 to 90% of microbes in soil are attached to solid surfaces, understanding the specific components of soil that contribute to NTM growth and maintenance in a geographic focal point for infection like Hawai'i is imperative (15). In this study, we performed microbiome and mineralogic studies and applied permuted feature importance approaches to predict soil components associated with NTM. We then tested the ability of these soil components to directly modulate the growth of native NTM isolates from Hawai'i *in vitro* and used high-powered microscopy to capture the capability of NTM to bind to these components.

The microbiome study demonstrated a trend toward lower alpha diversity in the NTM culture-positive samples, suggesting reduced richness of species compared to the NTM culture-negative samples (Fig. S4A). If the trend of lower alpha diversity in NTM culture-positive samples remains true when the sample size increases, this metric could potentially become a useful feature to predict NTM presence or absence in soil. Alpha diversity may also be linked to soil composition and competition for resources.

A variety of soil factors, or a combination of factors, could contribute to the presence or absence of environmental NTM. When analyzed as a single factor, soil pH was not found to be a significant driver for NTM diversity in this study (Fig. 1B), despite NTM showing a preference for acidic environmental conditions (pH 3 to 5) (e.g., acidic, brown water swamps; fulvic and humic acids; and peat-rich potting soils) (16–18). Most soils in Hawai'i have pH ranges from 4 to 8, but most are acidic due to the warm temperatures and high rainfall, leading to elevated pCO_2 values in the atmosphere. However, a primary driver of low pH in deeply weathered soils is the lack of base cations. Because we observed Hawai'i Island soil as more acidic than the other islands examined, future studies should further elucidate the role of soil pH to NTM growth.

A primary aim of this work was to determine important soil mineralogical features associated with NTM culture status by using machine learning tools to identify important features and then validating the impact of these minerals on NTM growth *in vitro*. Overall, soil feature distributions did not correlate directly with *in vitro* NTM culture assays. This may be a result of the limited power and the unbalanced outcome groupings. Yet, by using feature importance measures, we were able to identify gibbsite as a possible modulator of NTM growth (Fig. 2A) and confirmed that alone, pure gibbsite significantly inhibits the growth of *M. abscessus* and *M. chimaera* (Fig. 2B and C). Gibbsite is one of the mineral forms of aluminum hydroxide that forms the weathered surfaces of clays. Prior work detailing the soil composition of the Colombian Amazon has shown aluminum in clay possesses antibacterial activity against other microorganisms, including *Escherichia coli* (19). While gibbsite is common in tropical soils (20), the amount of gibbsite or its interaction with other minerals may influence the presence or absence of NTM in Hawai'i soil. Beyond the examination of aluminum as a single factor, the combination of aluminum and iron has been shown to increase the production of reactive oxygen species in prokaryotes, which can cause cell death (21). Noteworthy of discussion, the inhibitory effect of gibbsite on NTM growth was lost when incubated with soil containing gibbsite and halloysite (Fig. 2D and E). It is possible that the surface chemistry and crystal size of pure gibbsite change when in a complex mixture such as soil containing other minerals (e.g., halloysite). Similar discrepancies were also observed for *M. chimaera* incubated with pure kaolin or kaolinite-containing soil. Incubation of *M. chimaera* with pure kaolin did not alter CFU counts at the time points tested (Fig. 2C); however, significantly less *M. chimaera* was recovered

overtime when incubated in soil containing kaolinite (Fig. 2E). Besides kaolinite, it is possible the soil sample also contained other unidentified minerals or other factors that inhibited *M. chimaera* growth. It would be prudent to perform more detailed chemical analyses of these particular soils in the future.

The presence of iron in soil can promote NTM growth, and our feature predictions posit this is also true in Hawai'i soil (Fig. 3A). Our *in vitro* data indicate that not all iron oxide minerals such as maghemite, magnetite, and hematite impact the growth of NTM equally. For example, *M. abscessus* growth was facilitated in the presence of all iron oxides tested, particularly hematite (Fig. 3B), which was also associated with higher growth of *M. avium* (Fig. S7B) but with little impact on *M. chimaera* (Fig. 3C). Hematite has already been shown to promote the growth of soil-dwelling *Pseudomonas mendocina* by acting as an iron source *in vitro* (22). Because of the importance of iron equestration by NTM, it would be prudent for future work to dissect the role of *M. abscessus*, *M. chimaera*, and *M. avium* siderophores on iron sequestration from soil. Additionally, the impact of iron oxides on NTM biofilm development is an avenue for future study given the known effect of iron on the growth of *M. smegmatis* and *M. tuberculosis* biofilms (23, 24).

Manganese is an important minor element commonly found in basalts and other mafic rocks and is implicated as an inhibitory agent for NTM in soil. Although numerous manganese oxides and hydroxides (e.g., pyrolusite, manganite, and cryptomelane) have been identified, birnessite is one of the most common in soil (25). Birnessite demonstrated potent antibacterial activity against both SGM *M. chimaera* (Fig. 4B) and *M. avium* (Fig. S7C) but did not affect the growth of the RGM *M. abscessus* (Fig. 4A). *M. chimaera* growth was impaired in the presence of cryptomelane by the 96-h time point. Interestingly, the manganese oxide pyrolusite facilitated the growth of all three NTM species tested. In other studies, manganese oxide nanoparticles were found to exert antibacterial activity against *Vibrio cholerae*, *Shigella* species, and *E. coli*, and birnessite has been shown to inhibit pathogenic prions (26, 27). The role of manganese oxides/hydroxides in NTM growth in Hawaiian soils remains an open question. Additional work would be required to identify how manganese negatively or positively impacts NTM growth in the environment.

SEM images augment the culturing studies by illustrating the relationships between mineral substrates and NTM cells, although fixation and rinsing steps in mount preparations may not preserve a 1:1 relationship between cells and cell attachment versus abundances in culturing experiments. *M. abscessus* was seen in abundance attached to the surfaces of hematite grains and on the filter membrane of the mineral-free control culture, whereas it was not observed in the presence of birnessite and gibbsite (Fig. 5). Similar relationships were observed for *M. chimaera*. This species was found in the presence of hematite, although not in the relatively high proportions exhibited by *M. abscessus*, but was absent on gibbsite or birnessite (Fig. 5).

The absence of NTM in the presence of pure gibbsite (Fig. 2B and C) may be due to aluminum toxicity (19). In addition, gibbsite is very fine-grained, with crystallites $<1\ \mu$m in diameter (Fig. 5), which may preclude attachment to a single grain. Similarly, individual birnessite grains are very small and unfavorable for attachment. Presumably, some aspects of the surface chemistry of birnessite may also contribute to the inhibition of *M. chimaera* and *M. avium* in soil.

This study introduced the possibility that transition metals and oxide features in soil influence NTM growth *in vitro*. Future work should elucidate the various mechanisms used by NTM to evade the toxicity of soil factors to promote extended survival in the environment. For example, RGM, including *M. fortuitum* and *M. chelonae*, have been shown to resist exposure to transitional metals such as mercury through actions of protective mercuric reductases and organomercurial lyases (28, 29). In addition, the type VII secretion systems (e.g., ESX-3) of environmental mycobacteria have been associated with iron acquisition via mycobactin, a secreted iron chelator that promotes survival (30). Finally, it is possible NTM also utilize other siderophores, chelating proteins such as calprotectins, or structures similar to "zincosomes" (zinc-holding
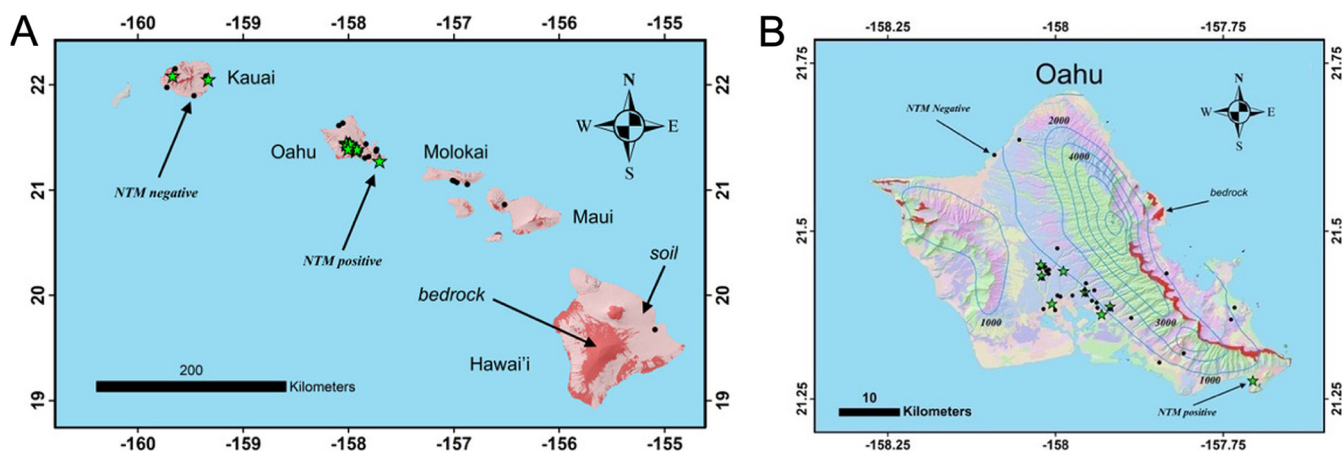
FIG 6 Hawai'i soil map. (A) Location of soil samples in the Hawaiian Islands, with NTM-positive (green stars) and NTM-negative soils (black dots) as indicated. (B) Map of Oahu indicating NTM-positive and -negative soils. Blue contours are mean annual rainfall (mm/yr). Red indicates the presence of bedrock at the surface and the other map colors represent various soil orders (48).

compartments) produced by *Mycobacterium tuberculosis*, as multifaceted mechanisms to protect from soil toxicity including control of uptake, oxidation, sequestration inside the bacteria, and efflux of toxic soil materials (31).

This study has some limitations. Soil samples were unequally collected from a limited number of sites across Oahu, Kauai, Hawai'i Island, Molokai, and Maui (Fig. 6). Collecting an increased number of soils that more widely and equally represent the different geographic areas across the islands would not only increase the limited sample size but will also provide a more complete study set to more robustly identify features that influence NTM growth. Increasing the number of NTM culture-positive samples with defined soil characteristics would also improve the balance of the data set and the overall feature selection performance. The addition of more samples would also increase the power of comparisons in the microbiome analysis. A single concentration of each mineral was used to compare across species and time points; however, the growth of NTM may be modulated with lower or larger amounts of compounds. Because soil is a complex mixture of many different components, we also cannot rule out the role of all other soil components (e.g., sodium, zinc, copper, and organic material) or other environmental factors such as rainfall and humidity in NTM growth and sustainability. Finally, because we were interested in studying *M. abscessus* and *M. chimaera*, clinically relevant NTM found in the lung, these experiments were performed at 37°C; however, soil temperature likely varies widely in the environment, and these results might change with lower incubation temperature.

In closing, this study is the first, to our knowledge, to characterize the soil composition in detail and relate that to NTM culture status. This study also identified important minerology features in Hawai'i soil using the application of machine learning tools, which were then validated *in vitro*. In addition, this study captured microscopy images of NTM binding to soil features. Because gibbsite and some of the manganese oxides were shown to decrease NTM growth and hematite, and pyrolusite promoted growth, it would be prudent to quantify these components and others in other soil samples globally in future work with subsequent translation of these findings to the presence or absence of clinically relevant NTM species in the environment.

MATERIALS AND METHODS

Soil samples and NTM isolates used in this study. In 2012, 65 different soil samples were collected from locations across Oahu, Kauai, Hawai'i Island, Molokai, and Maui, and NTM culture diversity from these samples was previously reported (8). A subset of 55 samples was used for downstream processing due to missing data, and the samples' collection sites are plotted in Fig. 6 based on global positioning system coordinates. The average rainfall of the sites ranged from less than 1,000 mm/year to 2,000 mm/year. Of note, this study did not consider soil types categorized by the USDA classification system. Of these soils, 13/65 (20%) were NTM culture positive. To assess the impact of soil minerals and components

TABLE 1 Information about the minerals used in this study

Mineral	Mineral group	Formula	Expt type
1:1 Clays	1:1 Clays	$Al_2Si_2O_5(OH)_4$	*In silico*
Halloysite	1:1 Clay (natural)	$Al_2Si_2O_5(OH)_4$	*In vitro*
Kaolinite	1:1 Clay (natural)	$Al_2Si_2O_5(OH)_4$	*In vitro*
Gibbsite	Clay (synthetic)	$Al(OH)_3$	Both
Magnetite	Fe-Ti oxide/hydroxide	Fe_3O_4	Both
Maghemite	Fe-Ti oxide/hydroxide	Fe_2O_3	Both
Hematite	Fe-Ti oxide/hydroxide	Fe_2O_3	Both
Ilmenite	Fe-Ti oxide/hydroxide	$FeTiO_3$	*In silico*
Goetithe	Fe-Ti oxide/hydroxide	$FeO(OH)$	*In silico*
Calcite/aragonite	Carbonate minerals	$CaCO_3$	*In silico*
Plagioclase	Feldspar	$NaAlSi_3O_8 \| CaAl_2Si_2O_8$	*In silico*
Pyrolusite	Mn oxide (natural)	MnO_2	*In vitro*
Cryptomelane	K, Mn oxide (natural)	$K(Mn)_8O_{16}$	*In vitro*
Birnessite	K, Mn oxide (synthetic)	$K(Mn)_2O_4 \cdot 1.5H_2O$	*In vitro*
Manganite	Mn oxide/hydroxide (natural)	$MnO(OH)$	*In vitro*

on NTM growth *in vitro*, two environmental Hawai'i NTM isolates were tested in the *in vitro* studies detailed herein, including 12-45-Sw-A-1 *Mycobacteroides abscessus* subsp. *abscessus* isolated from an Oahu household kitchen sink biofilm and 12-56-S-1-1 *M. chimaera* isolated from an Oahu household garden soil sample (8). *M. avium* subsp. *hominissuis* H87 isolated from an indoor sink faucet was also tested (32).

Microbiome analysis. Of the 55 soil samples, a subset that included 8 NTM culture-positive and 10 NTM culture-negative soils was subjected to microbiome profiling. DNA was obtained using the PowerSoil DNA isolation kit from MoBio Labs, Inc. (33). Small subunit ribosomal sequencing reads were generated on an Ion Torrent personal genome machine. The V4 region of the 16S rRNA gene was amplified from total extracted DNA using the following primers: 515F, 5'-GTGCCAGCMGCCGCGGTAA-3', and 806R, 5'-GGACTACHVGGGTWTCTAAT-3'. Sequencing reads were processed through Dada2 (version 1.6.0) to infer sequence variants in R (version 3.4.4) (34, 35). The Dada2 processing pipeline was adjusted to operate on ion torrent semiconductor data by adjusting the homopolymer gap penalty to −1 and increasing the band size parameter to 32 per instructions from the package creators. In addition to the Hawai'i samples, the sequencing run included a no-template control (NTC) to account for spurious amplification during the library preparation. Following sequence variant tabulation with Dada2, counts that remained in the NTC were deducted from the soil samples. The resulting samples had a mean of 22,000 sequence variants per sample with a maximum count of 30,173 and a minimum count of 9,214. Samples were rarified to the minimum count used to establish relative abundance values of sequence variants commonly used in community-level statistics and within the phyloseq R package (version 1.22.3) (36). Taxonomic identification of sequence variants was accomplished in Dada2 using a naive Bayesian classifier against a Dada2-formatted SILVA 128 database (37). Differential abundances of sequence variants by culture status was performed using a negative binomial model through DeSeq2 (version 1.18.1) (38). Genus-level counts of mycobacterium were split into two groups with equal membership using the discretize function of the arules package (version 1.6-1). Visualizations in R were performed with ggplot2 (version 2.2.1) embedded within the phyloseq package. Microbiome data and the code to replicate the figures are freely available on Github at https://github.com/Strong-Lab/NTM_Soil.

Soil pH and mineralogy. Soil, saprolite, and fresh rock pH values were measured by adding deionized water to dried material (crushed in the case of fresh rock) until the pore space was saturated and the surface glistened. A standard pH probe and meter were used, and a unique calibration for each sample was generated by measuring pH 4, 7, and 10 buffer solutions.

Minerals were quantified by using a Rigaku MiniFlex 600 X-ray diffractometer (XRD) employing copper radiation and a scintillation detector with a graphite monochromator as a practical rapid screening and characterization tool for complex soil mixtures. Mineral abundances were quantified by standard Rietveld methods embedded in the Rigaku PDXL2 software. Following filtering of columns with sparse information, the resulting matrix contained 11 features for examination, including magnetite, hematite, ilmenite, maghemite, gibbsite, carbonate minerals, quartz, pH, plagioclase, 1:1 clays, and goethite (Table 1).

Feature correlation analyses. Feature correlation analyses were used to identify and determine the strength of the correlation between features and response variables. Soil mineralogy was populated using 55 soil samples. The response variable tested was NTM culture status (culture positive or culture negative). Soil characteristics and culture status were imported into a pandas (version 0.20.3) DataFrame object in a Jupyter Notebook (version 4.3.0) using Python (version 3.6). The StandardScaler function from the scikit-learn package (version 0.19.1) was used to normalize soil characteristic percentages within each feature column. The Shapiro-Wilks function from the SciPy package (version 1.0.0) was used to test the normality of each column in both culture status groups. If either group rejected the null hypothesis, a nonparametric Wilcoxon signed-rank test was used to test for significance between NTM culture status. Otherwise, a *t* test with unequal variances was employed to test between the 2 distributions. Feature importance was calculated with the permutation importance function within eli5 (version 0.8.2). Feature values were shuffled in 1,000 permutations, creating an effect of removing the information from a given

feature on the performance of a classifier. Thus, features were assigned a mean decrease in accuracy (MDA) signifying how important a feature was to the accuracy of a machine learning model (Fig. S1). MDA features scores were represented in decimal format using Seaborn (version 0.9.0). The balance of samples in our model and the unexplained variance of NTM culture status limits the performance of a classification model and, thus, the overall values of the feature scores (39). The relationship of MDA scores was used to select important features for downstream *in vitro* growth assays. Feature scores changed slightly in each iteration. However, the ordering of importance and significance of the relationships between features remained intact. MDA scores and standard deviations were averaged into a group designated "all remaining features" when not the focus of the soil composition analysis. Feature importance scores only identified soil characteristics useful for accuracy of a machine learning classifier; however, feature importance did not indicate a significant correlation between the abundance of soil features and the outcome variable.

In vitro NTM growth assays in the presence of soil components and sterilized soil samples. General information for the individual minerals tested in this study is included in Table 1.

The HNL 12-48 soil sample was identified to be rich in kaolinite and free of halloysite and gibbsite. The RAP samples were recovered, by rappelling, from a sea cliff on the northern shoreline of the Kohala peninsula of the Big Island (40). These samples were selected due to the presence of significant quantities of gibbsite and halloysite. Synthetic gibbsite was provided by Barry Bickmore, Brigham Young University (BYU) research collections. Pure birnessite was synthesized by acid titration (41). Crushed hematite was obtained from the BYU research mineral collection. Kaolinite (product no. K1512) and halloysite (product no. 685445) were obtained from Sigma-Aldrich, and maghemite was obtained from U.S. Research Nanomaterials(CAS no. 1309-37-1). After completing a mineral dose-response assay for *M. abscessus* (Fig. S2) and *M. chimaera* (Fig. S3), 100 mg/ml of mineral was chosen for *in vitro* growth experiments. Soil samples were autoclaved at 132°C for 15 min, plated on standard Middlebrook 7H10 mycobacterial culture agar (42), and incubated at 37°C for a minimum of 3 days to ensure sample sterility. All particles were suspended to 100 mg/ml in standard mycobacterial culture broth media Middlebrook 7H9 (43) supplemented with 10% albumin-dextrose-catalase (ADC), 2% glycerol, and 0.05% Tween 80. These reagents, both autoclaved and nonsterile, were also characterized with the Rigaku MiniFlex using the CapWow capillary spinner sample holder. Small samples were loaded into 1-mm Kapton tubes and rotated in the X-ray beam, effectively creating a random orientation during analysis.

One milliliter of all suspensions in low-bind microcentrifuge tubes was inoculated with 1×10^5 CFU/ml of 12-45-Sw-A-1 *M. abscessus* or 5×10^5 CFU/ml of 12-56-S-1-1 *M. chimaera* or *M. avium* H87 and incubated on a rotating stand at 37°C (44, 45). The same concentrations of NTM were added to 1 ml 7H9 broth as untreated controls. At the 1-, 24-, 48-, and 96-h time points postinoculation, the cultures were serially diluted in 7H9 broth, and the dilutions were plated in duplicate onto 7H10 agar supplemented with 10% ADC and incubated at 37°C. To determine changes in CFU, the plates were counted 3 days postincubation for *M. abscessus* and 10 to 14 days postincubation for *M. chimaera* and *M. avium*.

Scanning electron microscopy. SEM images were obtained for *M. abscessus* and *M. chimaera* grown for 48 h in the presence of hematite, gibbsite, birnessite, and untreated controls. Suspensions were filtered through a 0.2-μm Isopore (catalog no. R8MA21491) membrane filter. Next, the samples were fixed with 3% glutaraldehyde in 0.1 M cacodylate buffer (pH 7.3) for 16 h, rinsed with distilled water three times for 10 min, treated with 1% OsO_4 at 4°C for 16 h, and rinsed again with distilled water. Samples were dehydrated by rinsing for 10 min with ethanol at concentrations of 30, 50, 70, 80, 90, 96, and 100% at 25°C, followed by acetone rinses at 30, 50, and 100% concentrations. Samples were then dried with a critical point dryer, mounted on aluminum SEM stubs with double-sided carbon tape, and coated with a gold-palladium alloy. An FEI Apreo scanning electron microscope at BYU obtained 6-megapixel secondary-electron images in a low vacuum with a 10-kV and 0.1-nA beam.

In vitro data analysis. Differences in log_{10} CFU/ml between NTM cultures exposed to clays/minerals and unexposed/control cultures were estimated using analysis of variance (ANOVA) models with robust sandwich covariance estimators. Separate models were run for each NTM species (*M. abscessus*, *M. chimaera*, and *M. avium*) at each postexposure time point (1 h, 48 h, 96 h, and, in some experiments, 24 h). Comparisons were made between clay soils, synthetic clays, iron-bearing minerals, and manganese-bearing minerals. ANOVA analyses were performed in R (46) version 3.6.3. Robust covariance estimation was performed using the sandwich package (47) version 2.5-1.

SUPPLEMENTAL MATERIAL

Supplemental material is available online only.

SUPPLEMENTAL FILE 1, PDF file, 2.8 MB.

REFERENCES

1. Honda JR, Virdi R, Chan ED. 2018. Global environmental nontuberculous mycobacteria and their contemporaneous man-made and natural niches. Front Microbiol 9:2029. https://doi.org/10.3389/fmicb.2018.02029.

2. Walsh CM, Gebert MJ, Delgado-Baquerizo M, Maestre FT, Fierer N. 2019. A global survey of mycobacterial diversity in soil. Appl Environ Microbiol 85:e01180-19. https://doi.org/10.1128/AEM.01180-19.

3. Lahiri A, Kneisel J, Kloster I, Kamal E, Lewin A. 2014. Abundance of Mycobacterium avium ssp. hominissuis in soil and dust in Germany - implications for the infection route. Lett Appl Microbiol 59:65–70. https://doi.org/10.1111/lam.12243.

4. De Groote MA, Pace NR, Fulton K, Falkinham JO, III. 2006. Relationships between Mycobacterium isolates from patients with pulmonary mycobacterial infection and potting soils. Appl Environ Microbiol 72:7602–7606. https://doi.org/10.1128/AEM.00930-06.

5. Fujita K, Ito Y, Hirai T, Kubo T, Maekawa K, Togashi K, Ichiyama S, Mishima M. 2014. Association between polyclonal and mixed mycobacterial Mycobacterium avium complex infection and environmental exposure. Annals ATS 11:45–53. https://doi.org/10.1513/AnnalsATS.201309-297OC.

6. Fujita K, Ito Y, Hirai T, Maekawa K, Imai S, Tatsumi S, Niimi A, Iinuma Y, Ichiyama S, Mishima M. 2013. Genetic relatedness of Mycobacterium avium-intracellulare complex isolates from patients with pulmonary MAC disease and their residential soils. Clin Microbiol Infect 19:537–541. https://doi.org/10.1111/j.1469-0691.2012.03929.x.

7. Adjemian J, Olivier KN, Seitz AE, Holland SM, Prevots DR. 2012. Prevalence of nontuberculous mycobacterial lung disease in U.S. Medicare beneficiaries. Am J Respir Crit Care Med 185:881–886. https://doi.org/10.1164/rccm.201111-2016OC.

8. Honda JR, Hasan NA, Davidson RM, Williams MD, Epperson LE, Reynolds PR, Smith T, Iakhiaeva E, Bankowski MJ, Wallace RJ, Jr, Chan ED, Falkinham JO, III, Strong M. 2016. Environmental nontuberculous mycobacteria in the Hawaiian islands. PLoS Negl Trop Dis 10:e0005068. https://doi.org/10.1371/journal.pntd.0005068.

9. Adjemian J, Olivier KN, Seitz AE, Falkinham JO, III, Holland SM, Prevots DR. 2012. Spatial clusters of nontuberculous mycobacterial lung disease in the United States. Am J Respir Crit Care Med 186:553–558. https://doi.org/10.1164/rccm.201205-0913OC.

10. Chou MP, Clements AC, Thomson RM. 2014. A spatial epidemiological analysis of nontuberculous mycobacterial infections in Queensland, Australia. BMC Infect Dis 14:279. https://doi.org/10.1186/1471-2334-14-279.

11. Lipner EM, Knox D, French J, Rudman J, Strong M, Crooks JL. 2017. A geospatial epidemiologic analysis of nontuberculous mycobacterial infection: an ecological study in Colorado. Ann Am Thorac Soc 14:1523–1532. https://doi.org/10.1513/AnnalsATS.201701-081OC.

12. Vitousek P. 2006. Ecosystem science and human-environment interactions in the Hawaiian archileago. J Ecology 94:510–521. https://doi.org/10.1111/j.1365-2745.2006.01119.x.

13. Barton CD, Karathanasis AD. 2002. Clay minerals, p 187–192. In Lal R (ed), Encyclopedia of soil science. Marcel Dekker, New York, NY.

14. Nelson ST, Tingey DG, Selck B. 2013. The denudation of ocean islands by ground and surface waters: the effects of climate, soil thickness, and water contact times on Oahu, Hawaii. Geochim et Cosmochim 103:276–294. https://doi.org/10.1016/j.gca.2012.09.046.

15. Nannipieri P, Ascher J, Ceccherini MT, Landi L, Pietramellara G, Renella G. 2003. Microbial diversity and soil functions. Eur J Soil Science 54:655–670. https://doi.org/10.1046/j.1351-0754.2003.0556.x.

16. Kirschner RA, Jr, Parker BC, Falkinham JO, III. 1992. Epidemiology of infection by nontuberculous mycobacteria. Mycobacterium avium, Mycobacterium intracellulare, and Mycobacterium scrofulaceum in acid, brown-water swamps of the southeastern United States and their association with environmental variables. Am Rev Respir Dis 145:271–275. https://doi.org/10.1164/ajrccm/145.2_Pt_1.271.

17. Portaels F, Pattyn SR. 1982. Growth of mycobacteria in relation to the pH of the medium. Ann Microbiol 133:213–221.

18. Bodmer T, Miltner E, Bermudez LE. 2000. Mycobacterium avium resists exposure to the acidic conditions of the stomach. FEMS Microbiol Lett 182:45–49. https://doi.org/10.1111/j.1574-6968.2000.tb08871.x.

19. Londono SC, Hartnett HE, Williams LB. 2017. Antibacterial activity of aluminum in clay from the Colombian Amazon. Environ Sci Technol 51:2401–2408. https://doi.org/10.1021/acs.est.6b04670.

20. Galán E. 2006. Genesis of clay minerals, p 1129–1162. In Bergaya F,

Theng BKG, Lagaly G (ed), Developments in clay science, vol. 1. Elsevier, Oxford, UK. https://doi.org/10.1016/S1572-4352(05)01042-1.

21. Exley C, Mold MJ. 2015. The binding, transport and fate of aluminium in biological cells. J Trace Elem Med Biol 30:90–95. https://doi.org/10.1016/j.jtemb.2014.11.002.

22. Hersman LE, Forsythe JH, Ticknor LO, Maurice PA. 2001. Growth of Pseudomonas mendocina on Fe(III) (hydr)oxides. Appl Environ Microbiol 67:4448–4453. https://doi.org/10.1128/aem.67.10.4448-4453.2001.

23. Ojha A, Hatfull GF. 2007. The role of iron in Mycobacterium smegmatis biofilm formation: the exochelin siderophore is essential in limiting iron conditions for biofilm formation but not for planktonic growth. Mol Microbiol 66:468–483. https://doi.org/10.1111/j.1365-2958.2007.05935.x.

24. Ojha AK, Baughn AD, Sambandan D, Hsu T, Trivelli X, Guerardel Y, Alahari A, Kremer L, Jacobs WR, Jr, Hatfull GF. 2008. Growth of Mycobacterium tuberculosis biofilms containing free mycolic acids and harbouring drug-tolerant bacteria. Mol Microbiol 69:164–174. https://doi.org/10.1111/j.1365-2958.2008.06274.x.

25. Gilkes RJ, McKenzie RM. 1988. Geochemistry and mineralogy of manganese in soils, p 22–35. In Graham RD, Hannam RJ, Uren NC (eds), Manganese in soils and plants, vol. 33. Springer, Dordrecht, Netherlands. https://doi.org/10.1007/978-94-009-2817-6_3.

26. Chowdhury AN, Azam MS, Aktaruzzaman M, Rahim A. 2009. Oxidative and antibacterial activity of Mn3O4. J Hazard Mater 172:1229–1235. https://doi.org/10.1016/j.jhazmat.2009.07.129.

27. Russo F, Johnson CJ, Johnson CJ, McKenzie D, Aiken JM, Pedersen JA. 2009. Pathogenic prion protein is degraded by a manganese oxide mineral found in soils. J Gen Virol 90:275–280. https://doi.org/10.1099/vir.0.003251-0.

28. Steingrube VA, Wallace RJ, Jr, Steele LC, Pang YJ. 1991. Mercuric reductase activity and evidence of broad-spectrum mercury resistance among clinical isolates of rapidly growing mycobacteria. Antimicrob Agents Chemother 35:819–823. https://doi.org/10.1128/aac.35.5.819.

29. Steingrube VA, Murphy D, McMahon S, Chapman JS, Nash DR. 1975. The effect of metal ions on the atypical mycobacteria: growth and colony coloration. Zentralbl Bakteriol Orig A 230:223–236.

30. Siegrist MS, Unnikrishnan M, McConnell MJ, Borowsky M, Cheng TY, Siddiqi N, Fortune SM, Moody DB, Rubin EJ. 2009. Mycobacterial Esx-3 is required for mycobactin-mediated iron acquisition. Proc Natl Acad Sci U S A 106:18792–18797. https://doi.org/10.1073/pnas.0900589106.

31. Neyrolles O, Wolschendorf F, Mitra A, Niederweis M. 2015. Mycobacteria, metals, and the macrophage. Immunol Rev 264:249–263. https://doi.org/10.1111/imr.12265.

32. Zhao X, Epperson LE, Hasan NA, Honda JR, Chan ED, Strong M, Walter ND, Davidson RM. 2017. Complete genome sequence of Mycobacterium avium subsp. hominissuis strain H87 isolated from an indoor water sample. Genome Announc 5. https://doi.org/10.1128/genomeA.00189-17.

33. Epperson LE, Strong M. 2020. A scalable, efficient, and safe method to prepare high quality DNA from mycobacteria and other challenging cells. J Clin Tuberc Other Mycobact Dis 19:100150. https://doi.org/10.1016/j.jctube.2020.100150.

34. Gilbert JA, Jansson JK, Knight R. 2014. The Earth Microbiome project: successes and aspirations. BMC Biol 12:69. https://doi.org/10.1186/s12915-014-0069-1.

35. Callahan BJ, McMurdie PJ, Rosen MJ, Han AW, Johnson AJ, Holmes SP. 2016. DADA2: high-resolution sample inference from Illumina amplicon data. Nat Methods 13:581–583. https://doi.org/10.1038/nmeth.3869.

36. McMurdie PJ, Holmes S. 2013. phyloseq: an R package for reproducible interactive analysis and graphics of microbiome census data. PLoS One 8:e61217. https://doi.org/10.1371/journal.pone.0061217.

37. Quast C, Pruesse E, Yilmaz P, Gerken J, Schweer T, Yarza P, Peplies J, Glockner FO. 2013. The SILVA ribosomal RNA gene database project: improved data processing and web-based tools. Nucleic Acids Res 41:D590–6. https://doi.org/10.1093/nar/gks1219.

38. Love MI, Huber W, Anders S. 2014. Moderated estimation of fold change and dispersion for RNA-seq data with DESeq2. Genome Biol 15:550. https://doi.org/10.1186/s13059-014-0550-8.

39. Louppe G, Wehenkel L, Sutera A, Geurts P. 2013. Understanding variable importances in forests of randomized trees, p 431–439. In Burges CJC, Bottou L, Welling M (ed), Proceedings of the 26th International Conference on Neural Information Processing Systems, vol 1. Curran

Associates Inc., Red Hook, NY. https://papers.nips.cc/paper/4928 -understanding-variable-importances-in-forests-of-randomized-trees.

40. Sowards K, Nelson ST, McBride JH, Bickmore B, Heizler MT, Tingey DG, Rey KA, Yaede JR. 2018. A conceptual model for the rapid weathering of tropical ocean islands: a synthesis of geochemistry and geophysics, Kohala Peninsula, Hawaii, USA. Geosphere 14:1324–1342. https://doi .org/10.1130/GES01642.1.

41. McKenzie RM. 1971. The synthesis of birnessite, cryptomelane, and some other oxides and hydroxides of manganese. Mineral Mag 38:493–502. https://doi.org/10.1180/minmag.1971.038.296.12.

42. Middlebrook G, Cohn ML. 1958. Bacteriology of tuberculosis: laboratory methods. Am J Public Health Nations Health 48:844–853. https://doi .org/10.2105/ajph.48.7.844.

43. Dubos RJ, Middlebrook G. 1947. Media for tubercle bacilli. Am Rev Tuberc 56:334–345.

44. Malcolm KC, Caceres SM, Honda JR, Davidson RM, Epperson LE, Strong M, Chan ED, Nick JA. 2017. Mycobacterium abscessus displays fitness for fomite transmission. Appl Environ Microbiol 83:e00562-17. https://doi .org/10.1128/AEM.00562-17.

45. Kim E, Kinney WH, Ovrutsky AR, Vo D, Bai X, Honda JR, Marx G, Peck E, Lindberg L, Falkinham JO, III, May RM, Chan ED. 2014. A surface with a biomimetic micropattern reduces colonization of Mycobacterium abscessus. FEMS Microbiol Lett 360:17–22. https://doi.org/10.1111/1574 -6968.12587.

46. R Core Team. 2020. R: a language and environment for statistical computing. R Foundation for Statistical Computing, Vienna, Austria. https:// www.R-project.org/.

47. A Z. 2004. Econometric computing with HC and HAC covariance matrix estimators. J Statistical Software 11:1–17. https://doi.org/10.18637/jss .v011.i10.

48. US Department of Agriculture. 2020. The twelve orders of soil taxonomy. US Department of Agriculture, Washington, DC. https://www.nrcs.usda .gov/wps/portal/nrcs/detail/soils/edu/?cid=nrcs142p2_053588.